

Vibration analysis of single-walled carbon nanotubes conveying nanoflow embedded in a viscoelastic medium using modified nonlocal beam model

M. HOSSEINI¹⁾, M. SADEGHI-GOUGHARI²⁾,
S. A. ATASHIPOUR³⁾, M. EFTEKHARI⁴⁾

¹⁾ *Department of Mechanical Engineering
Sirjan University of Technology
78137-33385 Sirjan, I.R., Iran
e-mail: hosseini@sirjantech.ac.ir*

²⁾ *Department of Mechanical Engineering
College of Technology of Sirjan
Shahid Bahonar University of Kerman
76169-14111 Kerman, I.R., Iran
e-mail: sadeghi.moslem87@gmail.com*

³⁾ *Department of Mechanical Engineering
Isfahan University of Technology
84156-83111 Isfahan, I.R., Iran
e-mail: sa.atashipour@me.iut.ac.ir*

⁴⁾ *Department of Mechanical Engineering
Yazd University
Yazd, I.R. Iran
e-mail: malihe_eftekhari@yahoo.com*

IN THIS STUDY, THE VIBRATION AND STABILITY ANALYSIS of a single-walled carbon nanotube (SWCNT) conveying nanoflow embedded in biological soft tissue are performed. The effects of nano-size of both fluid flow and nanotube are considered, simultaneously. Nonlocal beam model is used to investigate flow-induced vibration of the SWCNT while the small-size effects on the flow field are formulated through a Knudsen number (Kn), as a discriminant parameter. Pursuant to the viscoelastic behavior of biological soft tissues, the SWCNT is assumed to be embedded in a Kelvin–Voigt foundation. Hamilton’s principle is applied to the energy expressions to obtain the higher-order governing differential equations of motion and the corresponding higher-order boundary conditions. The differential transformation method (DTM) is employed to solve the differential equations of motion. The effects of main parameters including Kn , nonlocal parameter and mechanical behaviors of the surrounding biological medium on the vibrational properties of the SWCNT are examined.

Key words: single-walled carbon nanotube, small size effects, Knudsen number, nonlocal parameter, viscoelastic medium, differential transformation method.

1. Introduction

DISCOVERED BY IJIMA [1], CARBON NANOTUBES (CNTs) are effectively slender cylinders of graphite. CNTs have unique electronic, mechanical, thermal, fluid-transport and gas storage properties [2–5]. These exceptional properties have made CNTs to play an essential role in the wide range of applications in all areas of nanotechnology, such as nanofluidics and nanomedicine. In the field of nanofluidics, CNTs can be used as nanopipes for conveying fluid as well as nanocontainers for gas storage [6]. In the field of nanomedicine, CNTs can be used as matrices for compounds simulating neural growth, as pharmaceutical excipients for creating versatile drug delivery systems [7] and as biological sensors [8]. In drug delivery systems, single-walled carbon nanotubes (SWCNTs) are used to act as nanochannels for delivering drug into target cells [9], provided that SWCNTs should be embedded in biological soft tissue of the body. Mechanically, soft tissues are generally modeled by viscoelastic mediums [10]. Amongst several viscoelastic models, the Kelvin-Voigt model, a simple mechanical model composed of parallel spring and dashpot, is usually employed to simulate viscoelastic behavior [11].

Improvement in efficiency of these nanofluidics and nanobiological devices is dependent on a thorough understanding of their mechanical behaviors [12, 13]. The significance of this has transformed the dynamic analysis of CNTs with internal flowing to be an active subject of researches in past years.

As one of the first studies in this field, Yoon *et al.* [14] studied the effect of flow velocity on the vibrational behaviors of CNTs conveying fluid. They showed that this effect becomes more prominent especially for suspended, longer and larger inner-most radius CNTs at higher-flow velocity. They also revealed that the existence of an elastic medium can reduce the influence of internal flow on the resonant frequencies. They employed the classical beam theory to model and analyze the vibrational characteristics of CNTs conveying fluid. In addition, there has been an extensive research on the dynamic analysis of nanotubes conveying fluid by taking advantage of the classical beam theory, e.g., the researches done by KHOSRAVIAN *et al.* [15], REDDY *et al.* [16], WANG *et al.* [17], CHANG and LEE [18] and NATSUKI *et al.* [19].

As the size of CNTs is remarkably small, the material microstructure, i.e., the small size effects, becomes more significant so that they cannot be ignored anymore [20, 21]. At small length scales, utilizing the classical continuum beam model for analysis of nanostructures may cause unwanted errors; therefore, the usage of non-classical continuum theories, including internal material length scale parameter is inevitable [13]. Understanding the importance of employing non-local elasticity theory for small scale structures, a number of researchers have reported on static, dynamic and stability analyses of nanostructures [22–28].

Nonlocal elasticity theory was implemented to investigate the small-size effect on thermal vibration response of an embedded carbon nanotube based on Timoshenko's beam theory by AMIRIAN *et al.* [22]. Study on the effect of nonlocal scale on the dynamics of fluid conveying nanotubes was initiated by LEE and CHANG [23] and have been improved by other studies, e.g., [24, 25]. They concluded that the critical flow velocity and nanostructure stiffness of nanotubes with supported ends can be decreased by the increase in the value of nonlocal parameter. In all of the studies discussed so far, the governing equations of motion constructed for nanotube conveying fluid were presented to be of the fourth-order. Recently, however, it has been proved that these earlier studies were based on the partial nonlocal elasticity theory [26] and, as discussed by LIM *et al.* [27], under these circumstances the consequent governing equations of motion are not in equilibrium state. Taking advantage of nonlocal elasticity theory, LIM [28] presented the new equilibrium conditions and derived a modified nonlocal beam model in which the higher-order differential governing equation and the corresponding higher-order boundary conditions were presented. He also showed that the nanostructure stiffness is consistently enhanced by increasing the value of nonlocal parameter.

Based on the exact nonlocal stress model, WANG [26] developed a modified nonlocal beam model with the higher-order differential terms to analyze the vibration and stability properties of nanotubes conveying fluid. He also provided a new comprehension of the effect of nanoscale parameter on the vibration and stability of nanotubes conveying fluid.

On the other hand, in a nanoscale fluid structure interaction (FSI) problems, the small-size effects on the flow field become significantly important and the assumption of no-slip boundary conditions between the fluid flow and nanotube walls is no longer valid [29]. RASHIDI *et al.* [29] considered the small-size effects on the flow field to investigate the instability of CNTs conveying fluid. They devised a dimensionless parameter, called velocity correction factor (VCF) as a function of Kn to modify the FSI governing equations. It was found that for passage of gas through a nanotube, ignoring the small-size effects on the flow field in a nanoscale FSI problem might generate erroneous results. By considering the small size effects of viscosity of fluid flow, KAVIANI and MIRDAMADI [30] modified the parameter VCF introduced by RASHIDI *et al.* [29]. They revealed that this new formulation of VCF generated different results as compared to the case where nanosized fluid viscosity had been ignored in slip boundary conditions. MIRRAMEZANI and MIRDAMADI [31] investigated the effects of nonlocal elasticity and Kn on FSI in carbon nanotube conveying fluid. They revealed that the nonlocal parameter had more effect than Kn on the reduction of critical flow velocities of a liquid nanoflow, however in a gas nanoflow, the situation was totally different and Kn could cause more reduction in critical flow velocities. In the

previous studies on the effects of nanosize of fluid flow on the dynamics of nanotube conveying nanoflow, the classical continuum beam theory [29, 30] or the partial nonlocal beam theory [31] were employed for modeling nanotubes while the higher-order terms for both differential governing equations and boundary conditions were ignored.

As for the literature published so far, it is noted that several methods have been used to solve the FSI problems, such as Galerkin's method [29, 32], generalized differential quadrature method (GDQM) [33], general differential quadrature rule (GDQR) [26], etc. In this study, the differential transformation method (DTM) is employed to investigate the free vibration of SWCNT conveying nanoflow. The DTM was first proposed by ZHOU [34] for solving linear and non-linear initial value problems in electrical circuit analysis. Taking advantage of DTM, many investigations used this method to solve linear and nonlinear engineering problems, e.g., [35–38]. As was shown by NI *et al.* [39], DTM has high precision and computational efficiency in the vibration analysis of pipes conveying fluid. In fact, DTM is a semi-analytical method for solving differential equations, which is based on Taylor's series expansion. Taking advantage of some efficient transformation rules, DTM is used to convert the governing differential equations of motion into a set of algebraic equations.

The main objective of this paper is to present a nanoscale FSI model for analyzing the vibration and stability of a SWCNT conveying nanoflow embedded in biological soft tissue. For this purpose, a nanoscale FSI model is developed that considered the effects of nano-size of both fluid flow and nanotube simultaneously, in order to acquire a more exact forecast of the vibrational and stability properties of a SWCNT conveying nanoflow. Also, Kelvin-Voigt's viscoelastic model is employed to consider the effects of the biological medium on the stability of embedded SWCNT conveying fluid. Then, DTM, as an efficient numerical method, is employed to solve the obtained higher-order governing equations of motion. Numerical results are presented in graphical form to investigate the influence of Kn , nonlocal parameter and viscoelastic medium on the vibrational characteristics of SWCNT conveying fluid.

2. Derivation of the equations of motion

2.1. Nanoflow model

The Knudsen number, i.e., the ratio of mean free path to a characteristic length of problem geometry, is utilized as a discriminant parameter for identification of flow regime. Based on Kn , four flow regimes can be classified [40]: 1) continuum flow regime ($0 < Kn < 10^{-3}$), 2) slip flow regime ($10^{-3} < Kn < 10^{-1}$), 3) transition flow regime ($10^{-1} < Kn < 10$) and 4) free molecular flow regime ($Kn > 10$). In a nanoscale FSI problem, Kn may be larger than 10^{-3} and consequently, the

assumption of no-slip boundary conditions is invalid, therefore the Navier–Stokes continuum equations should be modified for the slip flow regime [29].

BESKOK and KARNIADAKI [41] suggested a slip velocity model to consider the slip boundary conditions in nanoflow field as

$$(2.1) \quad V_s - V_w = \left(\frac{2 - \sigma_v}{\sigma_v} \right) \left(\frac{Kn}{1 - bKn} \right) \left(\frac{\partial v_x}{\partial n} \right),$$

where V_s is the slip flow velocity near the CNT wall surface, V_w is the axial rigid body solid wall velocity, v_x is the axial flow velocity through the nanotube, n is the outward normalized unit normal vector to the CNT wall surface, σ_v is tangential momentum accommodation coefficient which is considered to be 0.7 for most practical purposes and b is a general slip coefficient. By choosing $b = -1$, one can make the effect of slip conditions as accurate as a second-order term. It should be noted that Eq. (2.1) can be valid for the entire Knudsen flow regime.

RASHIDI *et al.* [29] used the popular Navier–Stokes equations through the nanotube complemented with a second-order term for slip boundary conditions proposed by Eq. (2.1) and derived a velocity correction factor (VCF) as a function of Kn . They defined the VCF as the ratio of the average flow velocity through the nanotube considering slip boundary conditions (U_{slip}), to the average flow velocity through the nanotube incorporating no-slip boundary conditions (U) as

$$(2.2) \quad VCF \triangleq \frac{U_{\text{slip}}}{U} = (1 + aKn) \left(4 \left(\frac{2 - \sigma_v}{\sigma_v} \right) \left(\frac{Kn}{1 + Kn} \right) + 1 \right),$$

where a is a coefficient which can be varied from zero to a constant value, as follows [40]:

$$(2.3) \quad a = a_0 \frac{2}{\pi} [\tan^{-1}(a_1 Kn^B)].$$

The values of $a_1 = 4$ and $B = 0.4$ are some empirical parameters and a_0 is defined as [40]

$$(2.4) \quad a_0 = \frac{64}{3\pi \left(1 - \frac{4}{b}\right)},$$

where the parameter b in Eq. (2.4) is the same as b in Eq. (2.1). Here, a correction factor for average velocity is used to connect the continuum flow theory to the nanoflow model. It is noteworthy to mention that the slip velocity model (Eq. (2.1)) and the velocity correction factor (Eq.(2.4)) can be used for both nanoliquid and nanogas flows [29]. Although liquid flows have a small Kn , because the mean free path of liquid molecules could not reach large amount, however a gas flow could reach any Kn continuously and typically are sensitive to small size effects [29].

2.2. Nonlocal stress model

As illustrated in [42, 43], at nanoscale the material properties are size-dependent which makes the material microstructure significantly important. In this situation, the continuum beam model needs to be modified; this may be achieved by using the nonlocal stress field theory. In accordance with this theory [44, 45], the nonlocal stress field at a reference point \mathbf{x} is assumed to be a function of the strain field at all the other points in the body as

$$(2.5) \quad \sigma(\mathbf{x}) = \int_v \mathfrak{R}(|\mathbf{x}' - \mathbf{x}|, \tau) \mathbf{t}(\mathbf{x}') d\mathbf{x}',$$

where $\mathbf{t}(\mathbf{x})$ is the local macroscopic stress tensor at the reference point \mathbf{x} , $\mathfrak{R}(|\mathbf{x}' - \mathbf{x}|, \tau)$ is the kernel function, $|\mathbf{x}' - \mathbf{x}|$ is the distance between points and τ is a dimensionless nanolength scale:

$$(2.6) \quad \tau = \frac{e_0 a}{L},$$

in which a and L are the internal and external characteristic lengths, respectively, and e_0 is a material constant. It should be noted that, when $\tau \rightarrow 0$, the effect of strain at points $\mathbf{x} \neq \mathbf{x}'$ can be neglected. Because of special integral in the nonlocal relation, solving the nonlocal elasticity problems is mathematically difficult. For this reason and according to Eringen [44, 45], the nonlocal constitutive relation with a certain approximation error can be expressed as

$$(2.7) \quad (1 - \tau^2 L^2 \nabla^2) \sigma = \mathbf{t}.$$

In a one-dimensional Euler–Bernoulli nanobeam, the nonlocal constitutive equation can be expressed as [46]

$$(2.8) \quad \sigma = \sum_{n=1}^{\infty} \tau^{2(n-1)} \frac{d^{2(n-1)} \varepsilon}{dx^{2(n-1)}},$$

where σ and ε are dimensionless nonlocal stress and strain, respectively.

2.3. FSI governing equation

Consider a uniform nanotube of length L with bending rigidity of EI and mass per unit length m embedded in a viscoelastic medium, as shown in Fig. 1. Suppose that nanofluid with mass per unit length M and with steady axial slip flow velocity U_{slip} flows through the nanotube. The nanotube is assumed to be slender with lateral motion $W(X, T)$, where X and T are axial and time coordinates, respectively. The governing equation and the corresponding boundary conditions can be derived via the extended Hamilton principle. This can be

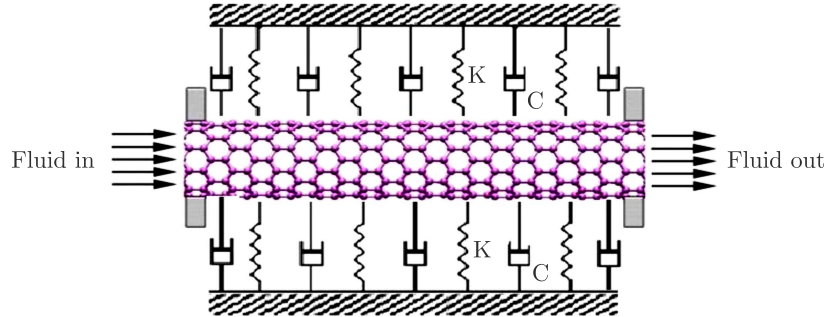


FIG. 1. Configuration of SWCNT conveying nanoflow embedded in a viscoelastic medium.

formulated as

$$(2.9) \quad \int_{t_1}^{t_2} (\delta E_k - \delta E_e + \delta W^{ext}) dt = 0,$$

where E_k and E_e denote the kinetic and potential energies, respectively and δW^{ext} is virtual work due to the non-conservative external forces. For free vibration of nanotubes conveying fluid, the kinetic energy is given by

$$(2.10) \quad E_k = \frac{1}{2}M \int_0^L \left[U_{slip}^2 + \left(\frac{\partial W}{\partial T} + U_{slip} \frac{\partial W}{\partial X} \right)^2 \right] dX + \frac{1}{2}m \int_0^L \left(\frac{\partial W}{\partial T} \right)^2 dX.$$

With considering the average velocity correction factor, Eq. (2.2), and introducing dimensionless axial, lateral and time coordinates as

$$x = \frac{X}{L}, \quad w = \frac{W}{L}, \quad t = \frac{T}{L^2} \left(\frac{EI}{M+m} \right)^{1/2}$$

respectively, Eq. (2.10) can be rewritten as

$$(2.11) \quad E_k = \frac{1}{2}ML \int_0^1 \left\{ \frac{EI}{ML^2} (VCF)^2 u^2 + \left[\frac{1}{L} \left(\frac{EI}{M+m} \right)^{1/2} \frac{\partial w}{\partial t} + \left(\frac{EI}{M} \right)^{1/2} (VCF) \frac{u}{L} \frac{\partial w}{\partial x} \right]^2 \right\} dx + \frac{m}{L} \left(\frac{EI}{m+M} \right) \int_0^1 \left(\frac{\partial w}{\partial t} \right)^2 dx,$$

the variation of kinetic energy can be obtained as

$$(2.12) \quad \int_{t_1}^{t_2} \delta E_k dt = \int_{t_1}^{t_2} \frac{EI}{L} \left\{ - \int_0^1 \left(\frac{\partial^2 w}{\partial t^2} + 2(VCF)u\sqrt{\beta} \frac{\partial^2 w}{\partial x \partial t} + (VCF)^2 u^2 \frac{\partial^2 w}{\partial x^2} \right) \delta w dx + \left[\left((VCF)u\sqrt{\beta} \frac{\partial w}{\partial t} + (VCF)^2 u^2 \frac{\partial w}{\partial x} \right) \delta w \right]_0^1 \right\} dt,$$

where u and β are respectively dimensionless flow velocity with no-slip conditions and mass ratio,

$$(2.13) \quad u = \left(\frac{M}{EI} \right)^{1/2} UL, \quad \beta = \frac{M}{m + M}.$$

In the present study, the potential energy is composed of two terms: 1) strain energy of deformed nanotube expressed as “ E_{ep} ” and 2) potential energy due to the spring forces, stated as “ E_{es} ”; therefore, the variation of potential energy can be written as

$$(2.14) \quad \delta E_e = \delta E_{ep} + \delta E_{es}.$$

As discussed by LIM [28], the variation of strain energy of deformed nanotube can be finally expressed as

$$(2.15) \quad \delta E_{ep} = \frac{EI}{L} \int_0^1 \left[- \sum_{n=1}^{\infty} (2n-3) \tau^{2(n-1)} \frac{\partial^{2(n+1)} w}{\partial x^{2(n+1)}} \right] \delta w dx + \frac{EI}{L} \left[\sum_{n=1}^{\infty} (2n-3) \tau^{2(n-1)} \frac{\partial^{(2n+1)} w}{\partial x^{(2n+1)}} \delta w - \sum_{n=1}^{\infty} (2n-3) \tau^{2(n-1)} \frac{\partial^{2n} w}{\partial x^{2n}} \frac{\partial \delta w}{\partial x} + \sum_{n=1}^{\infty} (2n-1) \tau^{2n} \frac{\partial^{(2n+1)} w}{\partial x^{(2n+1)}} \frac{\partial^2 \delta w}{\partial x^2} + \dots \right]_0^1.$$

Regarding the Kelvin–Voigt viscoelastic model, the potential energy due to the spring forces and the virtual work due to the damping properties of soft

equation of motion and the corresponding boundary conditions can be rewritten in the final forms as

$$(2.21) \quad -\tau^2 \frac{\partial^6 w}{\partial x^6} + \frac{\partial^4 w}{\partial x^4} + (VCF)^2 u^2 \frac{\partial^2 w}{\partial x^2} + 2(VCF)u\sqrt{\beta} \frac{\partial^2 w}{\partial x \partial t} + \frac{\partial^2 w}{\partial t^2} + c \frac{\partial w}{\partial t} + kw = 0,$$

$$(2.22) \quad \begin{aligned} \frac{\partial^3 w}{\partial x^3} - \tau^2 \frac{\partial^5 w}{\partial x^5} + (VCF)^2 u^2 \frac{\partial w}{\partial x} + (VCF)u\sqrt{\beta} \frac{\partial w}{\partial t} &= 0 \quad \text{or } w = 0, \\ \frac{\partial^2 w}{\partial x^2} - \tau^2 \frac{\partial^4 w}{\partial x^4} &= 0 \quad \text{or } \frac{\partial w}{\partial x} = 0, \\ \frac{\partial^3 w}{\partial x^3} + 3\tau^2 \frac{\partial^5 w}{\partial x^5} &= 0 \quad \text{or } \frac{\partial^2 w}{\partial x^2} = 0. \end{aligned}$$

The boundary conditions considered in this study are:

(a) *pinned-pinned nanotube*:

$$(2.23) \quad \text{at } x = 0, 1, \quad w = 0, \quad \frac{\partial^2 w}{\partial x^2} = 0, \quad -\frac{\partial^2 w}{\partial x^2} + \tau^2 \frac{\partial^4 w}{\partial x^4} = 0.$$

b) *clamped-clamped nanotube*:

$$(2.24) \quad \text{at } x = 0, 1, \quad w = 0, \quad \frac{\partial w}{\partial x} = 0, \quad \frac{\partial^3 w}{\partial x^3} + 3\tau^2 \frac{\partial^5 w}{\partial x^5} = 0.$$

c) *clamped-pinned nanotube*:

$$(2.25) \quad \begin{aligned} \text{at } x = 0, \quad w = 0, \quad \frac{\partial w}{\partial x} = 0, \quad \frac{\partial^3 w}{\partial x^3} + 3\tau^2 \frac{\partial^5 w}{\partial x^5} &= 0, \\ \text{at } x = 1, \quad w = 0, \quad \frac{\partial^2 w}{\partial x^2} = 0, \quad -\frac{\partial^2 w}{\partial x^2} + \tau^2 \frac{\partial^4 w}{\partial x^4} &= 0. \end{aligned}$$

It should be noted that the above modified nonlocal beam model described in Eqs. (2.21) and (2.22) can be reduced to the classical continuum beam model by letting $\tau = 0$ and $Kn = 0$ ($VCF = 1$).

3. Differential transformation method and solution methodology

The basic definitions and the application procedure of differential transformation method can be expressed as follows. Consider a function $f(x)$ which is analytic in a domain S and let $x = x_0$ represents any point in S . The function

$f(x)$ may be represented by a power series whose center is located at x_0 . The i th differential transformation of the function $f(x)$ is given as [34]

$$(3.1) \quad \bar{f}(i) = \frac{1}{i!} \left(\frac{d^i f(x)}{dx^i} \right)_{x=x_0},$$

while the inverse differential transformation method can be defined as

$$(3.2) \quad f(x) = \sum_{i=0}^{\infty} (x - x_0)^i \bar{f}(i).$$

It is proved that $\sum_{i=N+1}^{\infty} (x - x_0)^i \bar{f}(i)$ is very small and can be ignored when N is sufficiently large, so Eq. (3.2) can be rewritten as a finite series [39]:

$$(3.3) \quad f(x) = \sum_{i=0}^N (x - x_0)^i \bar{f}(i),$$

where the value of N depends on the convergence requirement conditions. Table 1 lists the basic mathematical operations related to DTM.

Table 1. Basic theorems of DTM for equations of motion.

Original functions	Transformed functions
$f(x) = g(x) \pm h(x)$	$\bar{f}(i) = \bar{g}(i) \pm \bar{h}(i)$
$f(x) = \lambda g(x)$	$\bar{f}(i) = \lambda \bar{g}(i)$
$f(x) = g(x) h(x)$	$\bar{f}(i) = \sum_{l=0}^i \bar{g}(i-l) \bar{h}(l)$
$f(x) = \frac{d^n g(x)}{dx^n}$	$\bar{f}(i) = \frac{(i+n)!}{i!} \bar{g}(i+n)$
$f(x) = x^m$	$\bar{f}(i) = \delta(i-m) = \begin{cases} 0 & \text{if } i \neq m, \\ 1 & \text{if } i = m \end{cases}$

3.1. DTM transformation of equation of motion

The solution of Eq. (2.21) is assumed to be in the form of:

$$(3.4) \quad w(x, t) = \tilde{w}(x)e^{\Omega t},$$

where Ω is the dimensionless eigenvalue. Substituting Eq. (3.4) into Eq. (2.21) yields:

$$(3.5) \quad -\tau^2 \frac{d^6 \tilde{w}}{dx^6} + \frac{d^4 \tilde{w}}{dx^4} + (VCF)^2 u^2 \frac{d^2 \tilde{w}}{dx^2} + 2(VCF)u\sqrt{\beta}\Omega \frac{d\tilde{w}}{dx} + \Omega^2 \tilde{w} + c\Omega \tilde{w} + k\tilde{w} = 0.$$

Using the transformation operations defined in Table 1 and taking the differential transformation of Eq. (3.5) at $x_0 = 0$, one may obtain:

$$(3.6) \quad -\tau^2(i+1)(i+2)(i+3)(i+4)(i+5)(i+6)\bar{w}(i+6) + (i+1)(i+2)(i+3)(i+4)\bar{w}(i+4) + (i+1)(i+2)(VCF)^2 u^2 \bar{w}(i+2) + 2(i+1)(VCF)u\sqrt{\beta}\Omega \bar{w}(i+1) + (\Omega^2 + c\Omega + k)\bar{w}(i) = 0,$$

where $\bar{w}(i)$ is the transformed functions of $\tilde{w}(x)$. Rearranging Eq. (3.6), the equation of motion can be transformed into the following recurrence relation as

$$(3.7) \quad \bar{w}(i+6) = \frac{(\Omega^2 + c\Omega + k)\bar{w}(i)}{\tau^2(i+1)(i+2)(i+3)(i+4)(i+5)(i+6)} + \frac{2(VCF)u\sqrt{\beta}\Omega \bar{w}(i+1)}{\tau^2(i+2)(i+3)(i+4)(i+5)(i+6)} + \frac{(VCF)^2 u^2 \bar{w}(i+2)}{\tau^2(i+3)(i+4)(i+5)(i+6)} + \frac{\bar{w}(i+4)}{\tau^2(i+5)(i+6)}.$$

3.2. DTM transformation of boundary conditions

Similarly, by substituting Eq. (3.4) into Eqs. (2.23)–(2.25) and applying DTM by using the theorems introduced in Table 1, the DTM transformation of boundary conditions are given as follows:

(a) *pinned-pinned nanotube:*

$$(3.8) \quad \bar{w}(0) = 0,$$

$$(3.9) \quad \bar{w}(2) = 0,$$

$$(3.10) \quad 2\bar{w}(2) - 24\tau^2 \bar{w}(4) = 0,$$

$$(3.11) \quad \sum_{i=0}^N \bar{w}(i) = 0,$$

$$(3.12) \quad \sum_{i=0}^N i(i-1)\bar{w}(i) = 0,$$

$$(3.13) \quad \sum_{i=0}^N [i(i-1) - i(i-1)(i-2)(i-3)\tau^2] \bar{w}(i) = 0.$$

(b) *clamped-clamped nanotube:*

$$(3.14) \quad \bar{w}(0) = 0,$$

$$(3.15) \quad \bar{w}(1) = 0,$$

$$(3.16) \quad 6\bar{w}(3) + 360\tau^2\bar{w}(5) = 0,$$

$$(3.17) \quad \sum_{i=0}^N \bar{w}(i) = 0,$$

$$(3.18) \quad \sum_{i=0}^N i\bar{w}(i) = 0,$$

$$(3.19) \quad \sum_{i=0}^N [i(i-1)(i-2) + 3\tau^2 i(i-1)(i-2)(i-3)(i-4)]\bar{w}(i) = 0.$$

(c) *clamped-pinned nanotube:*

$$(3.20) \quad \bar{w}(0) = 0,$$

$$(3.21) \quad \bar{w}(1) = 0,$$

$$(3.22) \quad 6\bar{w}(3) + 360\tau^2\bar{w}(5) = 0,$$

$$(3.23) \quad \sum_{i=0}^N \bar{w}(i) = 0,$$

$$(3.24) \quad \sum_{i=0}^N i(i-1)\bar{w}(i) = 0,$$

$$(3.25) \quad \sum_{i=0}^N [i(i-1) - i(i-1)(i-2)(i-3)\tau^2] \bar{w}(i) = 0.$$

3.3. Solution procedure and stability method

Combining Eq. (3.7) and those of the boundary conditions, we can obtain a solution to the problem in hand. In order to avoid the unnecessary repeating calculations, the solution procedure is explained for the pinned-pinned boundary condition.

From Eqs. (3.7)–(3.13), it can be seen that $\bar{w}(i)$, ($i = 6, 7, 8, \dots, N$) is a linear function of $\bar{w}(1)$, $\bar{w}(3)$, $\bar{w}(4)$, $\bar{w}(5)$. Using Eq. (3.7) $\bar{w}(i)$ can be worked out via an iterative procedure. Substituting $\bar{w}(i)$ into Eqs. (3.8)–(3.13) leads to an eigenvalue problem:

$$(3.26) \quad \begin{bmatrix} y_{11} & y_{12} & y_{13} & y_{14} \\ y_{21} & y_{22} & y_{23} & y_{24} \\ y_{31} & y_{32} & y_{33} & y_{34} \\ y_{41} & y_{42} & y_{43} & y_{44} \end{bmatrix} \begin{bmatrix} \bar{w}(1) \\ \bar{w}(3) \\ \bar{w}(4) \\ \bar{w}(5) \end{bmatrix} = 0,$$

where y_{ij} are associated with the dimensionless eigenvalue Ω and other parameters of system, corresponding to N . For a nontrivial solution, the determinant of the coefficient matrix vanishes. This leads to the characteristic equation of the problem as

$$(3.27) \quad \Delta(\tau, Kn, u, \beta, k, c; \Omega) = 0.$$

Therefore, the dimensionless eigenvalue Ω can be computed numerically from Eq. (3.27) as a function of Kn , τ and other parameters of nanotube system. Generally, Ω is a complex number where its imaginary component, $\text{Im}(\Omega)$, represents the dimensionless system frequency; while the real component, $\text{Re}(\Omega)$, is related to the damping of system denoted as the decaying rate of amplitude.

The system becomes unstable when the damping part of one of the eigenvalues becomes positive. The parameter values in which this condition takes place are often called critical parameter. In the case of divergence instability, the critical values of parameter are computed by setting $\Omega = 0$ in Eq. (3.27) and solving the resulting equation for an unknown parameter called divergence parameter. Thus, for given values of τ, Kn, β, k and c , the critical flow velocity at which divergence instability occurs can be determined.

4. Results and discussion

In this section, the DTM is utilized to simulate the vibrational behavior of SWCNT conveying nanoflow embedded in biological soft tissue. To this end, the material and geometrical properties of SWCNT are considered as, the outer radius $R_0 = 3$ nm, the wall thickness $h = 0.1$ nm, the aspect ratio $L/(2R_0) = 40$, the mass density $\rho_c = 2300$ kg·m⁻³ and the Young's modulus $E = 3.4$ TPa [10]. The fluid mass density is $\rho_{\text{water}} = 1000$ (kg·m⁻³) for water, and $\rho_{\text{air}} = 1.169$ (kg·m⁻³) for air. The elastic and damping properties of viscoelastic medium are taken to be $K = 0.1$ MPa and $C = 1.02 \times 10^{-4}$ Pa·s, respectively, [10].

4.1. Convergence study and validation

Successful application of numerical methods in engineering problems could be guaranteed only after their convergence study. As mentioned in Section 3, the precision of differential transformation method depends on the number of DTM terms (N) taken into account. The following inequalities present a criterion for determining the value of N to hold a desired accuracy [35]:

$$(4.1) \quad |\text{Im}(\Omega_j^N) - \text{Im}(\Omega_j^{N-1})| \langle \varepsilon; |\text{Re}(\Omega_j^N) - \text{Re}(\Omega_j^{N-1})| \langle \varepsilon,$$

where Ω_j^N denotes the j th estimated eigenvalue corresponding to N terms and Ω_j^{N-1} is associated with $(N-1)$ terms and ε is a small value. The computer package Maple is used to write a program for the expressions given by Eqs. (3.7)–(4.1).

At this stage, the convergence and accuracy of the DTM solution is verified and the effects of different parameters on the natural frequencies and divergence critical flow velocities are studied. Here, it should be noted that the critical flow velocity is the flow velocity at which the frequency and decaying rate reach to zero at the first mode. In fact, divergence critical flow velocities, u_{cr} , is independent of mass ratio, β , this is so because β is always associated with velocity-dependent terms in the equation of motion, while divergence represents a static instability [32].

Table 2 presents the dimensionless critical flow velocities without considering the nonlocal effect, the small size effects on the flow field and the viscoelastic medium $\tau = Kn = k = c = 0$, which exposes a classical pipe conveying fluid. As shown in this table, with increasing of N the results of DTM become closer to the solutions reported in [32] and a good agreement is obtained.

Table 2. Convergence and accuracy of the of the dimensionless critical flow velocity of the classical pipe conveying fluid for various numbers of DTM terms (N), ($\tau = Kn = k = c = 0$).

N	Dimensionless critical continuum flow velocity		
	pinned-pinned	clamped-pinned	clamped-clamped
10	3.0787	3.9394	4.8664
15	3.1416	4.4772	5.9807
20	3.1416	4.4934	6.2842
25	3.1416	4.4934	6.2831
30	3.1416	4.4934	6.2832
35	3.1416	4.4934	6.2832
Païdoussis [32]	π	≈ 4.49	2π

In Table 3, the results of dimensionless critical flow velocity of a SWCNT conveying nanoflow embedded in a Kelvin–Voigt foundation for different number of DTM terms (N) are presented for $\tau = 0.2$, $Kn = 0.1$, $k = 12.1$ and $c = 6.4$. Converged results up to six significant digits are obtained by using 45 DTM terms ($N = 45$). It can be seen that with increasing of N , the precision of DTM increases. Compared with the pinned end condition, the clamped end condition requires more terms adopted in the DTM.

Table 3. Convergence of the dimensionless critical flow velocity (u_{cr}) of the SWCNT conveying nanoflow embedded in a Kelvin–Voigt foundation for various numbers of DTM terms (N), ($\tau = 0.2$, $Kn = 0.1$, $k = 12.1$, $c = 6.4$).

N	Dimensionless critical continuum flow velocity		
	pinned-pinned	clamped-pinned	clamped-clamped
10	2.249752	1.111117	–
15	2.125470	2.544861	–
20	2.125536	3.258014	–
25	2.125536	3.209115	5.052731
30	2.125536	3.209355	5.084570
35	2.125536	3.209355	5.084442
40	2.125536	3.209355	5.084442
45	2.125536	3.209355	5.084442

Table 4 shows the critical continuum flow velocity against Kn for simply supported nanotube and the DTM results are compared with the results reported by KAVIANI and MIRDAMADI [30]. In this table, the calculations are performed for the same parameters as reported by above reference. The parameter values are, $E = 1.0$ TPa, $h = 10$ nm, $R_0 = 50$ nm, $\rho_c = 2300$ kg · m⁻³, $L/(2R_0) = 500$, and $\rho_{air} = 1.169$ kg · m⁻³. The results are derived based on the classical beam model ($\tau = 0$) and for $k = c = 0$. The numerical results illustrate an excellent agreement with the results of [30].

Table 4. Convergence and accuracy of critical continuum flow (air) velocity (m/s) against Kn for simply supported nanotube conveying fluid for various numbers of DTM terms (N), ($\tau = k = c = 0$).

N	Kn										
	0	0.2	0.4	0.6	0.8	1	1.2	1.4	1.6	1.8	2
15	1327.7	496.5	298.7	211.2	162.3	131.2	109.8	94.26	82.45	73.19	65.75
20	1393.0	520.9	313.4	221.6	170.3	137.7	115.2	98.90	86.50	76.79	68.99
25	1395.4	521.8	313.9	222.0	170.6	137.9	115.4	99.07	86.65	76.92	69.10
30	1395.4	521.8	313.9	222.0	170.6	137.9	115.4	99.07	86.65	76.92	69.10
Kaviani and Mirdamadi [30]	1395.4	521.8	313.9	222.0	170.6	137.9	115.4	99.07	86.65	76.92	69.10

The natural frequencies of SWCNT conveying nanoflow are dependent on the fluid velocity u . A SWCNT with zero fluid velocity behaves the same as a nanobeam structure, the natural frequencies of which can be obtained analytically.

ically. In order to show the accuracy of the DTM solution, the numerical results are presented to compare with those available in literature.

First, the lateral vibration of a classical nanobeam for $\tau = Kn = k = c = 0$, with zero fluid velocity is considered. The DTM results for the first four dimensionless natural frequencies are presented in Table 5 and compared with the exact solution of [47]. It is observed that, the results obtained by DTM are in very good agreement with the exact solutions for pinned-pinned, clamped-pinned and clamped-clamped boundary conditions.

Table 5. Comparison between the first four dimensionless natural frequencies of a classical nanobeam with different boundary condition ($u = \tau = Kn = k = c = 0$).

Boundary condition	Method	Frequency			
		$\text{Im}(\Omega_1)$	$\text{Im}(\Omega_2)$	$\text{Im}(\Omega_3)$	$\text{Im}(\Omega_4)$
Pinned-Pinned	DTM	9.8696	39.4784	88.8264	157.9137
	Exact solution [47]	9.8696	39.4784	88.8264	157.9137
Clamped-Pinned	DTM	15.4182	49.9649	104.2477	178.2697
	Exact solution [47]	15.4182	49.9649	104.2477	178.2697
Clamped-Clamped	DTM	22.3733	61.6728	120.9034	199.8594
	Exact solution [47]	22.3733	61.6728	120.9034	199.8594

Figure 2 shows the fundamental dimensionless vibration frequency of a pinned-pinned CNT conveying fluid as a function of the dimensionless flow velocity and the DTM results are compared with the results reported by WANG [26]. The results are computed for the case of $\tau = 0.1$, $Kn = k = c = 0$ and $\beta = 0.1$; as it is clear from this figure, a satisfactory agreement is found.

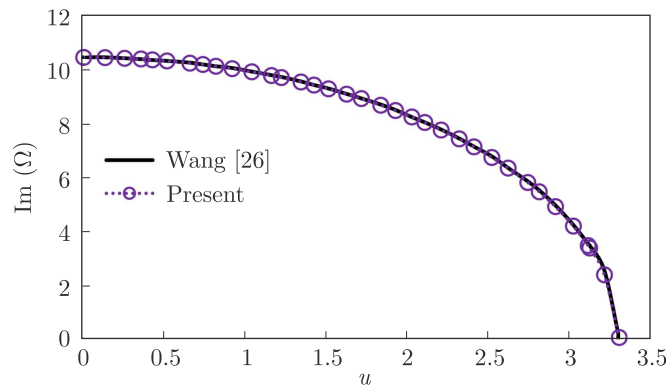


FIG. 2. The dimensionless natural frequency as a function of the dimensionless flow velocity for pinned-pinned nanotube, $\beta = 0.1$, $\tau = 0.1$, $Kn = k = c = 0$.

4.2. Frequency analysis

The vibrational frequencies of nanotubes conveying fluid depend on various parameters. Here, the influence of Knudsen number, nonlocal parameter and the mechanical characteristics of the surrounding biological medium have been examined in detail. As was discussed before in this nanoscale FSI study, the vibrational behaviors of system are examined in both the gas and liquid flows. In order to highlight the effects of aforementioned parameters, wherever the effect of Kn is important or disputable, the gas flow has been considered as the fluid flow; whereas, the liquid flow (denoted by zero Knudsen number) is considered wherever the effects of other parameters have been discussed.

The dimensionless frequency and damping parts of fundamental eigenvalues of a simply supported SWCNT are shown as a function of the dimensionless internal flow velocity in Fig. 3a and 3b, respectively. The results are presented

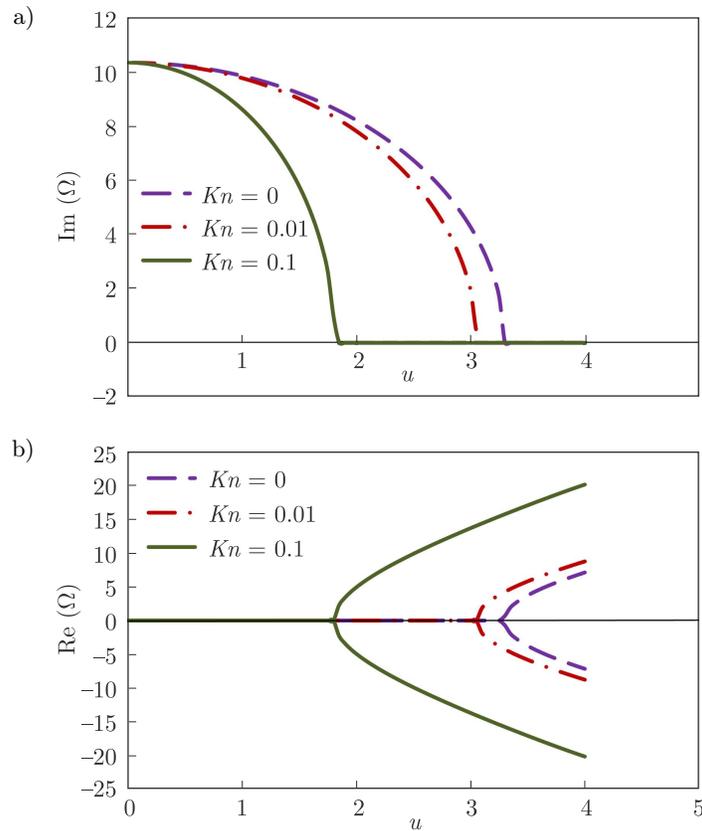


FIG. 3. Effect of the Kn on the dimensionless frequency and damping parts of the simply supported SWCNT conveying nanoflow for $\beta = 0.01$, $\tau = 0.1$ and $k = c = 0$; a) frequency part and b) damping part.

for different Kn , $Kn = 0, 0.01$ and 0.1 . For numerical calculations in this case, $\tau = 0.1$, $\beta = 0.01$ (air flow) and $k = c = 0$. It can be seen that by increasing Kn , the bending stiffness of SWCNT and the critical flow velocity decrease, so for nanogas flows, the small size effects on the flow field could extremely change the results.

In order to study the small scale effects on the solid SWCNT walls, the dimensionless frequency and damping parts of fundamental eigenvalues of a simply supported SWCNT are plotted as a function of the dimensionless internal flow velocity for three different nonlocal parameters, $\tau = 0, 0.1$ and 0.2 (Figs. 4a and 4b). For numerical calculation in this case, $\beta = 0.86$ (water flow), $k = 12.1$, $Kn = 0$ and $c = 6.4$. According to Fig. 4, the nonlocal effect tends to increase the critical flow velocity as well as the bending stiffness of SWCNT conveying nanoflow.

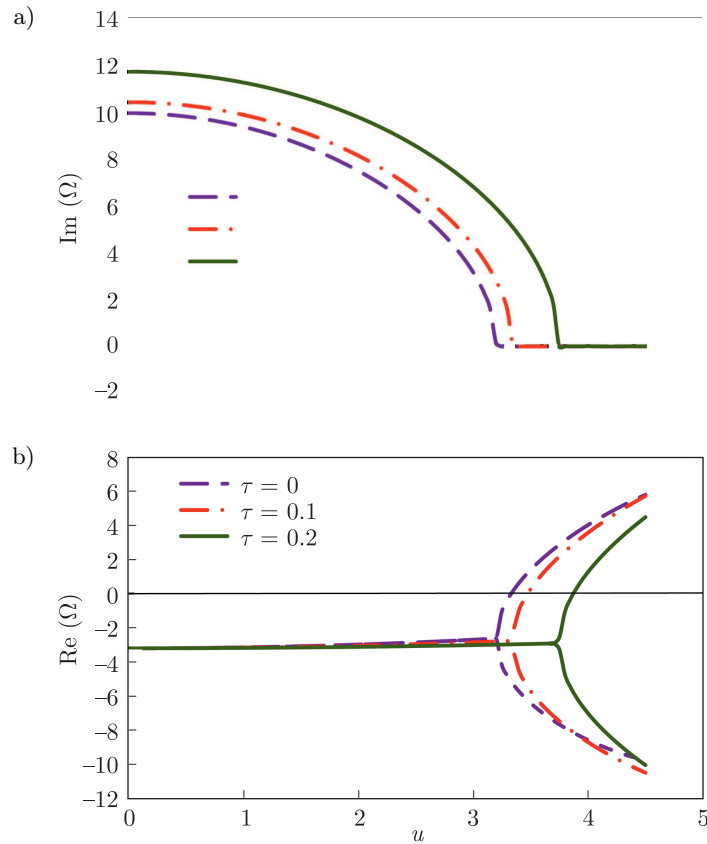


FIG. 4. Effect of the nonlocal parameter on the dimensionless frequency and damping parts of the simply supported SWCNT conveying nanoflow for $\beta = 0.86$, $Kn = 0$, $k = 12.1$ and $c = 6.4$; a) frequency part and b) damping part.

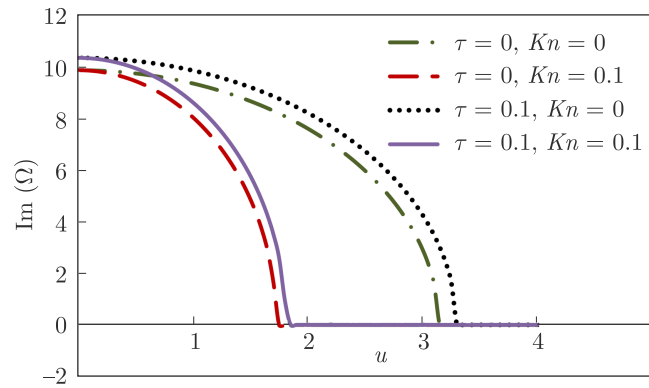


FIG. 5. Effect of the nonlocal parameter and Knudsen number simultaneously on the dimensionless frequency of the simply supported SWCNT conveying nanoflow for $\beta=0.01$, $k=c=0$.

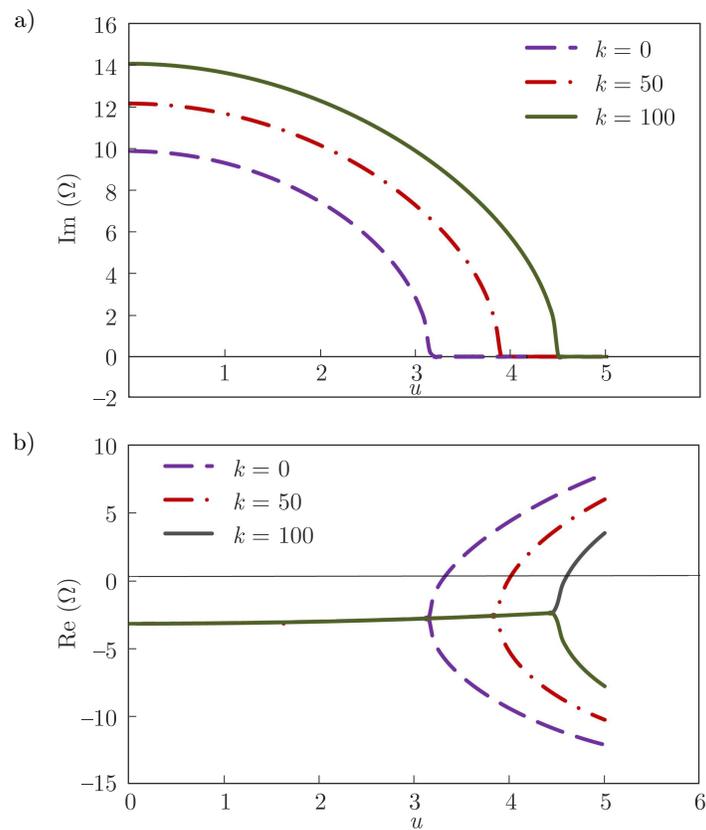


FIG. 6. The dimensionless frequency and damping parts of the simply supported SWCNT conveying nanoflow as a function of the dimensionless flow velocity for different value of dimensionless elastic parameter, $\beta = 0.86$, $Kn = 0$, $\tau = 0.1$ and $c = 6.4$; a) frequency part and b) damping part.

Thus, to explore the importance of simultaneous consideration of the aforementioned effects, i.e., the small size effects of both fluid and nanotube, the results of different models are compared with the present modified model (Fig. 5). According to this figure, ignoring any of those effects in a nanoscale FSI problem may generate erroneous results.

In the case of $\tau = 0.1$, $Kn = 0$, $\beta = 0.86$ (water flow) and $c = 6.4$, Figs. 6a and 6b, show the dimensionless frequency and damping parts of the fundamental eigenvalues of a simply supported SWCNT conveying nanoflow, respectively, for different dimensionless elastic parameters $k = 0$, $k = 50$, $k = 100$. It can be seen that by increasing the elasticity of the biological medium, the critical flow velocity increases.

Figures 7a and 7b illustrate the effect of damping coefficient c on the dimensionless frequency and damping parts of fundamental eigenvalues of the simply

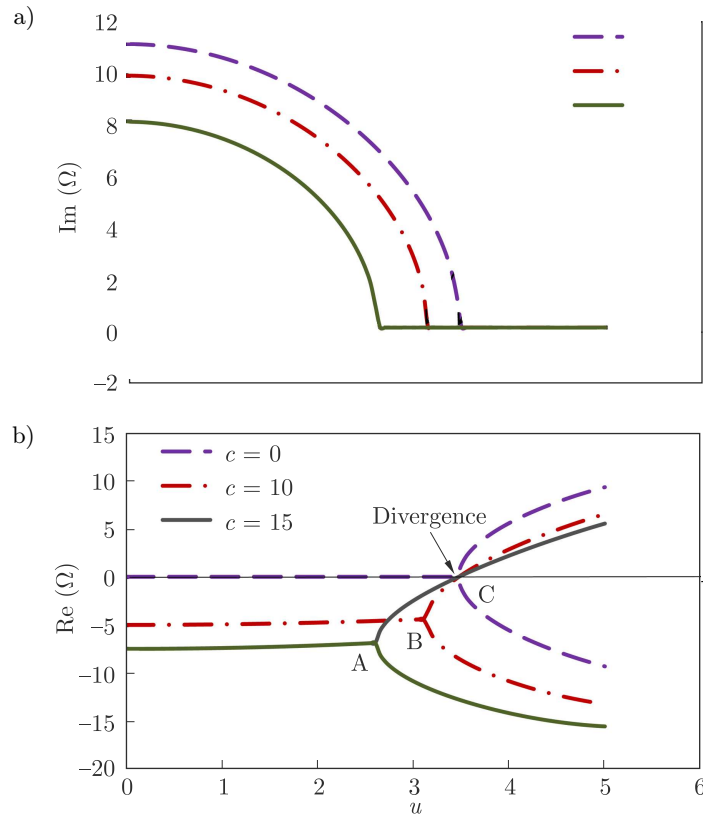


FIG. 7. The dimensionless frequency and damping parts against the dimensionless flow velocity for a pinned-pinned SWCNT conveying nanoflow for different values of dimensionless damping parameter, $\beta = 0.86$, $\tau = 0.1$, $Kn = 0$ and $k = 12.1$; a) frequency part and b) damping part.

supported SWCNT conveying nanoflow, respectively. Here, the results are presented for different dimensionless damping parameters, $c = 0$, $c = 10$ and $c = 15$. In this case, $\tau = 0.1$, $k = 12.1$, $Kn = 0$ and $\beta = 0.86$ (water flow). According to Fig. 7, the damping property of surrounding biological medium tends to decrease the bending stiffness of SWCNT conveying nanoflow. However it can be seen that the critical flow velocity for divergence instability is independent of damping coefficient, as far as divergence is a static behavior. In the other words, between the points A, B and C in Fig. 7, only in point C divergence occurs, because both the imaginary and the real parts of eigenvalue reach zero in this point.

4.3. Stability analysis

Another important aspect of dynamic analysis of nanotubes conveying nanoflow is the prediction of critical flow velocity u_{cr} . Similar to the natural frequencies, the critical flow velocities depend on several factors including the boundary conditions, the nonlocal parameter, the small size effects of flow field and the viscoelastic behaviors of the foundation.

The influence of nonlocal parameter on the critical flow velocities for simply supported SWCNT is presented in Fig. 8. The results are presented for classical and modified nonlocal beam models. For numerical calculations in this case, $Kn = 0$ and $k = c = 0$. From this figure, it is clear that the critical flow velocity predicted by the modified nonlocal model increases with stronger nonlocal effects which is higher than the classical value. The graphical results illustrate an excellent agreement with the results of WANG [26]. In this figure u_{cr_c} shows critical flow velocity for classical beam models.

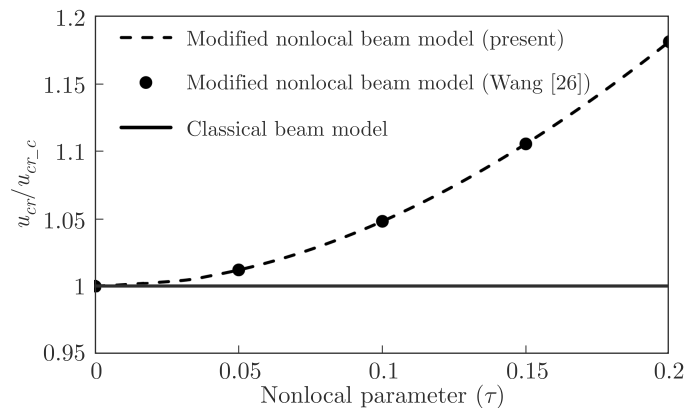


FIG. 8. The dimensionless critical flow velocity as a function of τ , predicted by modified nonlocal or classical beam model for $Kn = k = c = 0$ and pinned-pinned SWCNT.

Figures 9–11 represent the variation of critical flow velocity, u_{cr} , against Kn , while the effects of other parameters, i.e., boundary conditions, nonlocal parameter, and viscoelastic behaviors of the foundation, have been examined. In these figures, Kn changes from 0 to 10, the lines in these figures demonstrate the divergence boundaries. As can be seen there is one stable zone as well as one divergence zone for any certain parameter. It can be seen that in the case of continuum flow regime ($0 < Kn < 10^{-3}$) such as a liquid flow, Kn is not large enough to change the critical flow velocity drastically and u_{cr} becomes almost constant vs. Kn , but the effects of other parameters under investigation are still important. In the nanoscale FSI problem, when we have

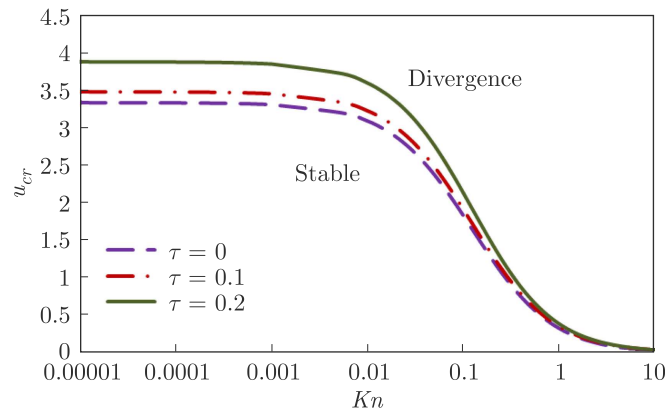


FIG. 9. The dimensionless critical flow velocity against the Kn with different values of the nonlocal parameter, for $k = 12.1$ and pinned-pinned SWCNT.

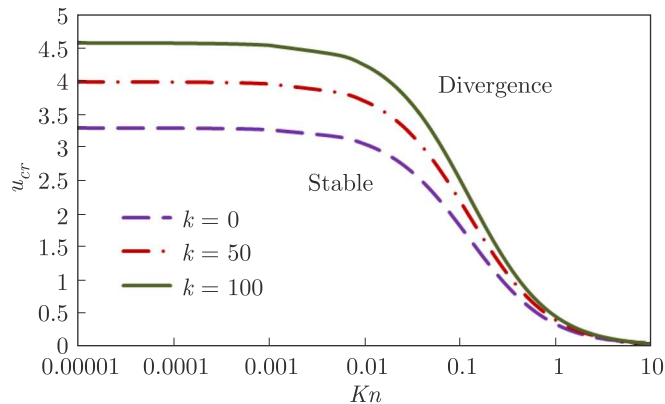


FIG. 10. The dimensionless critical flow velocity against the Kn with different values of the dimensionless elastic parameter for $\tau = 0.1$ and pinned-pinned SWCNT.

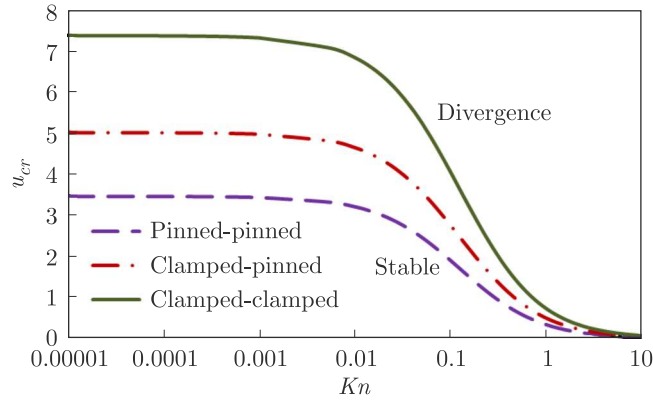


FIG. 11. The dimensionless critical flow velocity against the Kn with different type of boundary conditions for $\tau = 0.1$, $k = 12.1$.

gas flows as fluid flows such as air, Kn may be larger than 0.001, so in this case two approximate FSI flow regimes can be classified, (1) $0.001 < Kn < 1$; (2) $Kn > 1$.

For $0.001 < Kn < 1$, the effects of Kn , the nonlocal parameter, the boundary conditions and the elastic property of surrounding biological soft tissue, on the critical flow velocity are significant. However, for $Kn > 1$, it is found that the Kn has the dominant effect. In the other words, influences of other parameters are reduced significantly after $Kn = 1$ and increasing the Knudsen number decreases the critical flow velocity considerably. For $Kn > 1$ the critical flow velocity tends to vanish and the effects of expected influential parameters on the critical flow velocity become faint. On the other hand when $Kn \rightarrow 1$ the critical flow velocity limits to zero and $Kn \approx 1$ can be reported as a critical parameter in this nanoscale FSI problem. This approximate flow regime classification in the nanoscale FSI problems provide a new understanding of the influence of remarkable parameters on the vibration characteristics of nanotubes conveying nanoflow.

5. Conclusions

In this paper, we presented a modified nanoscale FSI model for vibration and stability analysis of SWCNT conveying nanoflow embedded in biological soft tissue. We developed a modified model that incorporates the small-size effects of flow field and nanotube, simultaneously while the small-size effects on slip boundary conditions of nanoflow were formulated through the Knudsen number, as a discriminant parameter. Consideration of Kn effect led to a decrease

in both the natural frequencies and critical flow velocities. Besides, an increase in both natural frequencies and critical flow velocities emerged from considering the nanoscale effect on the solid CNT walls. Also, the effect of viscoelastic parameters corresponding to the surrounding biological soft tissue was examined. It was observed that by increasing the elastic parameter of viscoelastic model, the critical flow velocity increased; on the other hand, the damping property of surrounding biological medium tended to decrease the bending stiffness of SWCNT conveying nanoflow, while the critical flow velocity did not change. Finally, a classification based on different values of Kn was made with respect to the critical flow velocity:

1) $0 < Kn < 10^{-3}$. In this band, Kn is not large enough to change the critical flow velocity drastically but the effects of other parameters were important.

2) $10^{-3} < Kn < 1$. In this flow regime, both Kn and other parameters were important and remarkable on critical flow velocity.

3) $Kn > 1$. The critical flow velocity tended to vanish and the effects of expected influential parameters on critical flow velocity become faint. This classification was concluded by using the proposed modified model.

References

1. S. IJIMA, *Helical microtubules of graphitic carbon*, Nature, **354**, 56–58, 1991.
2. T.W. EBBESEN, *Carbon Nanotubes: Preparation and Properties*, CRC Press, New York, 1997.
3. S.C. FANG, W.J. CHANG, Y.H. WANG, *Computation of chirality- and size-dependent surface Young's moduli for single-walled carbon nanotubes*, Physics Letter A, **371**, 499–503, 2007.
4. G.E. GADD, M. BLACKFORD, S. MORICCA, N. WEBB, P.J. EVANS, A.M. SMITH, G. JACOBSEN, S. LEUNG, A. DAY, Q. HUA, *The world's smallest gas cylinders?*, Science, **277**, 933–936, 1997.
5. E.V. DIROTE, *Trends in Nanotechnology Research*, Nova Science Publishers, New York, 2004.
6. L. WANG, Q. NI, M. LI, *Buckling instability of double-wall carbon nanotubes conveying fluid*, Computational Material Science, **44**, 821–825, 2008.
7. M. FOLDVARI, M. BAGONLURI, *Carbon nanotubes as functional excipients for nano-medicines: II*, Drug delivery and biocompatibility issues, Nanomedicine: Nanotechnology, Biology and Medicine, **4**, 183–200, 2008.
8. S. SAWANO, T. ARIE, S. AKITA, *Carbon nanotube resonator in liquid*, Nano Letters, **10**, 3395–3398, 2010.
9. N. KHOSRAVIAN, H. RAFII-TABAR, *Computational modelling of a non-viscous fluid flow in a multi-walled carbon nanotube modelled as a Timoshenko beam*, Nanotechnology, **19**, 275703, 2008.

10. P. SOLTANI, M.M. TAHERIAN, A. FARSHIDIANFAR, *Vibration and instability of a viscous-fluid conveying single-walled carbon nanotube embedded in a visco-elastic medium*, Journal of Physics D: Applied Physics, **43**, 425401, 2010.
11. E. GHAVANLOO, M. RAFIEI, F. DANESHMAND, *In-plane vibration analysis of curved carbon nanotubes conveying fluid embedded in viscoelastic medium*, Physical Letters A, **375**, 1994-1999, 2011.
12. S. RINALDI, S. PRABHAKAR, S. VENGALLATOR, M.P. PAIDOUSSIS, *Dynamics of micro-scale pipes containing internal flow: damping, frequency shift, and stability*, Journal of Sound and Vibration, **329**, 1081-1088, 2010.
13. L. WANG, *Size-dependent vibration characteristics of fluid-conveying microtubes*, Journal of Fluids and Structures, **26**, 675-684, 2010.
14. J. YOON, C.Q. RU, A. MIODUCHOWSKI, *Vibration and instability of carbon nano-tubes conveying fluid*, Composites Science and Technology, **65**, 1326-1336, 2005.
15. N. KHOSRAVIAN, H. RAFII-TABAR, *Computational modelling of the flow of viscous fluids in carbon nanotubes*, Journal of Physics D: Applied Physics, **40**, 7046-7052, 2007.
16. C.D. REDDY, C. LU, S. RAJENDRAN, K.M. LIEW, *Free vibration analysis of fluid-conveying single-walled carbon nanotubes*, Applied Physics Letters, **90**, 133122, 2007.
17. L. WANG, Q. NI, M. LI, Q. QIAN, *The thermal effect on vibration and instability of carbon nanotubes conveying fluid*, Physica E, **40**, 3179-3182, 2008.
18. W. CHANG, H. LEE, *Free vibration of a single-walled carbon nanotube containing a fluid flow using the Timoshenko beam model*, Physical Letters A, **373**, 982-985, 2009.
19. T. NATSUKI, Q.Q. NI, M. ENDO, *Wave propagation in single- and double-walled carbon nanotubes filled with fluids*, Journal of Applied Physics, **101**, 034319, 2007.
20. S. GOVINDJEE, J.L. SACKMAN, *On the use of continuum mechanics to estimate the properties of nanotubes*, Solid State Communications, **110**, 227-230, 1999.
21. L. WANG, *Vibration and instability analysis of tubular nano- and micro-beams conveying fluid using nonlocal elastic theory*, Physica E, **41**, 1835-1840, 2009.
22. B. AMIRIAN, R. HOSSEINI-ARA, H. MOOSAVI, *Thermal vibration analysis of carbon nanotubes embedded in two-parameter elastic foundation based on nonlocal Timoshenko's beam theory*, Archives of Mechanics, **64**, 581-602, 2012.
23. H. LEE, W. CHANG, *Free transverse vibration of the fluid-conveying single-walled carbon nanotube using nonlocal elastic theory*, Journal of Applied Physics, **103**, 024302, 2008.
24. L. WANG, *Dynamical behaviors of double-walled carbon nanotubes conveying fluid accounting for the role of small length scale*, Computational Material Science, **45**, 584-588, 2009.
25. A. TOUNSI, H. HEIRECHE, E.A.A. BEDIA, *Comment on "Free transverse vibration of the fluid-conveying single-walled carbon nanotube using nonlocal elastic theory"*, Journal of Applied Physics, **105**, 126105, 2009.
26. L. WANG, *A modified nonlocal beam model for vibration and stability of nanotubes conveying fluid*, Physica E, **44**, 25-28, 2011.
27. C.W. LIM, J.C. NIU, Y.M. YU, *Nonlocal stress theory for buckling instability of nanotubes: new predictions on stiffness strengthening effects of nanoscales*, Journal of Computational and Theoretical Nanoscience, **7**, 2104-2111, 2010.

28. C.W. LIM, *On the truth of nanoscale for nanobeams based on nonlocal elastic stress field theory: equilibrium, governing equation and static deflection*, Applied Mathematics and Mechanics (English Ed.), **31**, 37–54, 2010.
29. V. RASHIDI, H.R. MIRDAMADI, E. SHIRANI, *A novel model for vibrations of nanotubes conveying nanoflow*, Computational Material Science, **51**, 347–352, 2012.
30. F. KAVIANI, H.R. MIRDAMADI, *Influence of Knudsen number on fluid viscosity for analysis of divergence in fluid conveying nano-tubes*, Computational Material Science, **61**, 270–277, 2012.
31. M. MIRRAHEZANI, H.R. MIRDAMADI, *Effects of nonlocal elasticity and Knudsen number on fluid–structure interaction in carbon nanotube conveying fluid*, Physica E, **44**, 2005–2015, 2012.
32. M.P. PAÏDOUSSIS, *Fluid-Structure Interactions: Slender Structures and Axial Flow*, vol. 1, Academic Press, London, 1998.
33. F. TORNABENE, A. MARZANI, E. VIOLA, *Critical flow speeds of pipes conveying fluid using the generalized differential quadrature method*, Advances in Theoretical and Applied Mechanics, **3**, 121–138, 2010.
34. J.K. ZHOU, *Differential Transformation and Its Applications for Electrical Circuits*, Huazhong University Press, Wuhan, China, 1986.
35. C.K. CHEN, S.H. HO, *Solving partial differential equations by two-dimensional differential transform method*, Applied Mathematics and Computation, **106**, 171–179, 1999.
36. S.H. HO, C.K. CHEN, *Free transverse vibration of an axially loaded non-uniform spinning twisted Timoshenko beam using differential transform*, International Journal of Mechanical Sciences, **48**, 1323–1331, 2006.
37. C. MEI, *Application of differential transformation technique to free vibration analysis of a centrifugally stiffened beam*, Computers and Structures, **86**, 1280–1284, 2008.
38. M. BALKAYA, M.O. KAYA, A. SAGLAMER, *Analysis of the vibration of an elastic beam supported on elastic soil using the differential transform method*, Archive of Applied Mechanics, **79**, 135–146, 2009.
39. Q. NI, Z.L. ZHANG, L. WANG, *Application of the differential transformation method to vibration analysis of pipes conveying fluid*, Applied Mathematics and Computation, **217**, 7028–7038, 2011.
40. G. KARNIADAKIS, A. BESKOK, N. ALURU, *Microflows and Nanoflows: Fundamentals and Simulation*, Springer, USA, 2005.
41. A. BESKOK, G.E. KARNIADAKI, *A model for flows in channels, pipes, and ducts at micro and nano scales*, Microscale Thermophysical Engineering, **3**, 43–77, 1999.
42. J. PEDDIESON, G.R. BUCHANAN, R.P. MCNITT, *Application of nonlocal continuum models to nanotechnology*, International Journal of Engineering Science, **41**, 305–312, 2003.
43. R. LI, G. KARDOMATEAS, *Thermal buckling of multi-walled carbon nanotubes by nonlocal elasticity*, Journal of Applied Physics, **74**, 399, 2007.
44. A.C. ERINGEN, *On differential equations of nonlocal elasticity and solutions of screw dislocation and surface waves*, Journal of Applied Physics, **54**, 4703–4710, 1983.
45. A.C. ERINGEN, *Nonlocal Continuum Field Theories*, Springer, New York, 2002.

46. C.W. LIM, C.M. WANG, *Exact variational nonlocal stress modeling with asymptotic higher-order strain gradients for nanobeams*, Journal of Applied Physics, **101**, 054312, 2007.
47. W.T. THOMSON, *Theory of Vibration with Applications*, Unwin Hyman Ltd., London, 1988.

Received June 5, 2013; revised version May 1, 2014.
